

Computer simulation of pressing a ceramic ball into elastic-plastic material

Stefan Berczyński¹, Daniel Grochała¹, Zenon Grządziel²

¹ West Pomeranian University of Technology, Faculty of Mechanical Engineering and Mechatronics
70-310 Szczecin, Aleja Piastów 19, e-mails: {stefan.berczynski; daniel.grochala}@zut.edu.pl

² Maritime University of Szczecin, Institute of Basic Technical Sciences
70-500 Szczecin, ul. Wały Chrobrego 1–2, e-mail: z.grzadziel@am.szczecin.pl

Key words: computer simulation, ceramic ball, elastic-plastic material, burnishing, Hertzian stresses, deformations, and contact

Abstract

This article describes distributions of stresses and strains created by pressing a ball with 80 HRC hardness into soft 35HRC steel, which occurs in the technological process of burnishing. We present a computer model and a solution developed with the Nastran FX program, based on the finite elements method. The validity of the model has been checked using a small force applied on the ball, within the range of elastic deformations, where Hertz formulas are applicable. Then computations have been made for a pressure force of 30 000 N, which corresponds to hardness testing conditions by the Brinell method. The dimensions of plastic indentations from simulations and experiments are compared.

Introduction

Pressing a hard ceramic ball into a soft material is the first phase of surface treatment by burnishing (Grochała, Berczyński & Grządziel, 2014). A deep knowledge of stress and strain distributions running perpendicular and parallel to the treated surface is essential in selecting technological parameters of burnishing (Grochała, 2011; Lopez et al., 2005; 2007). In the next phase, the burnishing elements are shifted.

The physical model

This article presents a computer simulation of the process of pressing a ball 10 mm in diameter, made of the ceramic material ZrO_2 (zirconium dioxide) that has properties similar to steel: Young's modulus, E , equal to 210 GPa, Poisson's ratio, ν , equal to 0.29. A 10 mm ball is forced into the center of a specimen base, 20 mm in diameter and 10 mm in height (Figure 1). The cylindrical specimen is made of steel, X42CrMo4, with these properties: Young's modulus, E , equal to 210 GPa, Poisson's ratio, ν , equal to 0.29. The ceramic ball is resistant to plastic deformations (very hard,

80 HRC), while the specimen being burnished is made of soft material subject to elastic and plastic deformations (hardness 35–40 HRC).

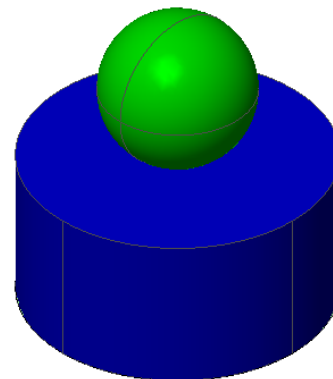


Figure 1. A physical model of a ball pressed into a cylindrical sample

The computer model

As the geometry of the objects and load are symmetrical, we took a section of a joint with 3° rotation angle to model the process of the ball pressing into the specimen material, as illustrated by Figure 2.

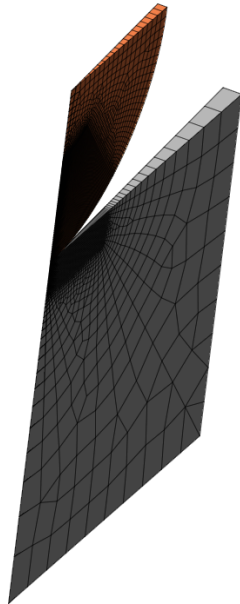


Figure 2. A section of a ball and cylinder divided into finite elements: 6,860 elements and 13,802 nodes

The ball section model is composed of 5,042 elements and 10,125 nodes. The cylindrical specimen model consists of 1,818 elements and 3,677 nodes. Around the point of contact of the ball and cylinder base we used a densified division into finite elements due to the occurrence of contact stresses (a side length of a finite element in this

area is 0.05 mm). All 3D elements were created by rotating 2D elements by a 3° angle around the joint axis. This resulted in 6-node elements fixed to the axis of rotation. Eight-node elements were created in the remaining volume.

Stress calculations in the elastic range at low pressure

To verify whether the adopted model is correct, we made calculations for low pressures to be able to determine whether the results of reduced stresses obtained directly from the Hertz formulae are valid for an elastic model. Instead of a calculator, we used the program HertzWin2.6.0 (Budynas & Nisbett, 2008; Deeg, 1992). The program makes use of the numerical integration method, and automatically presents the results in tables and diagrams. Figure 3 shows the calculations made by the program from physical model data, for the pressure force of 600 N.

The same problem was solved by means of the program Nastran FX (Nastran, 2010). The program is based on the finite elements method (FEM). Figure 4 presents a map of reduced stresses obtained with this program. Distributions of reduced stresses are clearly visible across the entire volume of the ball and the cylindrical specimen.



Figure 3. The results of calculations of the program HertzWin: ball radius 5 mm, force 600 N, with Young's modulus and Poisson's ratio the same for the ball and cylindrical specimen: $E = 210$ GPa, $\nu = 0.29$

The greatest values of these stresses do not occur on the contact surfaces, but at some distance from the surface, which can be seen in Figure 5, the diagram showing the stresses occurring along the symmetry axis of the joint. From a depth of 0.18 mm, the curves are overlapping.

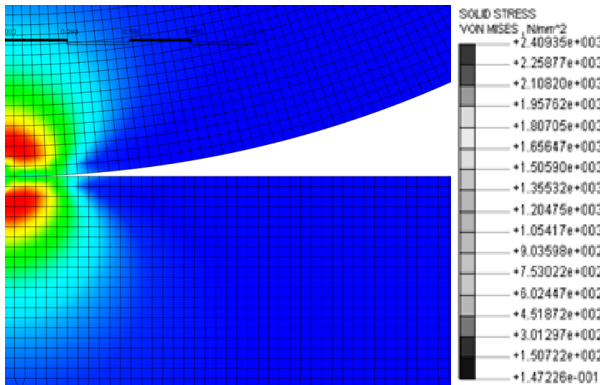


Figure 4. A map of reduced stresses obtained from Nastran FX calculations

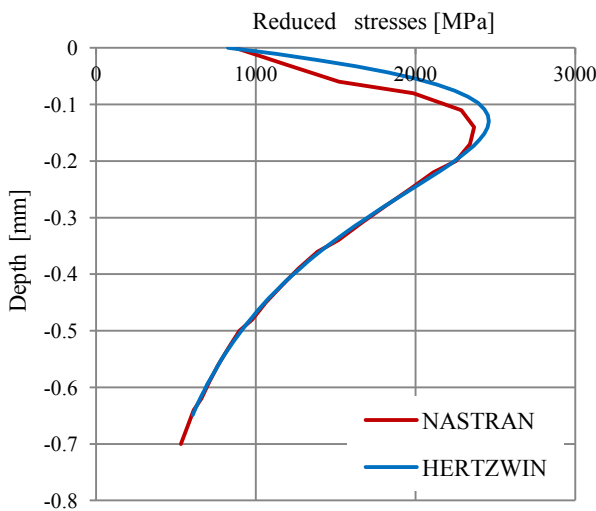


Figure 5. Distributions of reduced stress occurring along the axis of symmetry of the cylindrical specimen obtained by the programs HertzWin and Nastran FX

Calculations of residual stresses and strains

Calculations were made for stresses and strains created under a load of 30,000 N. This is the force to be imposed on the indenter in hardness measurements using a ball 10 mm in diameter. Because plastic strains occur under such conditions, the nonlinearities of the specimen material were accounted for. The diagram of stretching the material of the cylindrical specimen (steel X42CrMo4) is given in Figure 6.

This curve represents the stress σ as a function of relative elongation, ε , which was taken into account in the program Nastran FX. Figure 7 shows

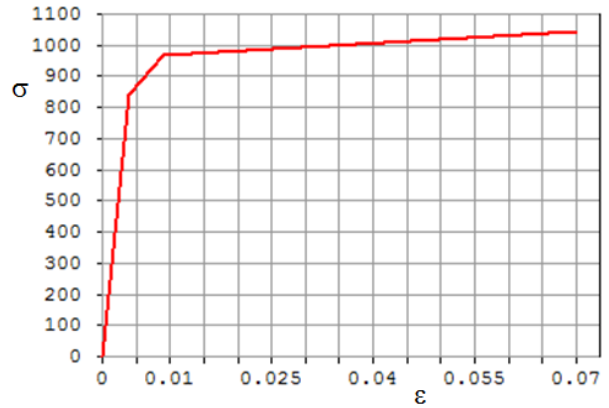


Figure 6. Diagram of stretching test of steel X42CrMo4

a map of stresses occurring in the ball and cylindrical specimen under a pressure of 30,000 N, as calculated by Nastran FX. The elastic stresses in the ball disappear once the load is removed, while the stresses in the cylindrical specimen are the sum of elastic and plastic stresses. Maximum reduced stresses in the ball occur 2 mm from the point of contact, and reach about 1550 MPa. Maximum reduced stresses in the cylindrical specimen occur on the contact surface and are equal to 1855 MPa.

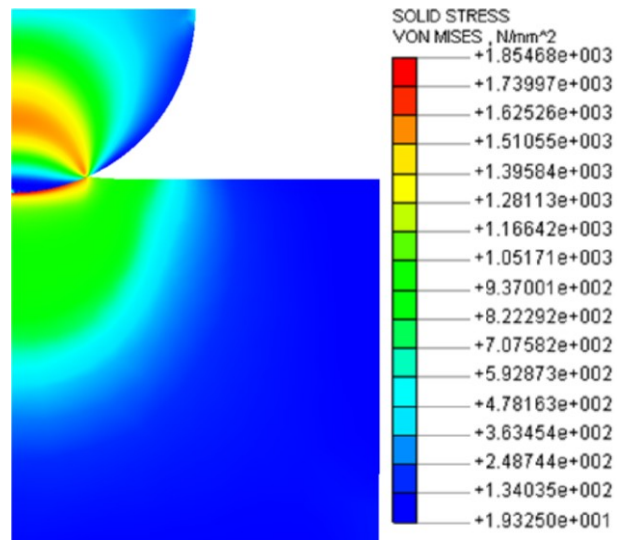


Figure 7. Reduced stresses in the ball and cylindrical specimen under a load of 30,000 N

Figure 8 presents a diagram of reduced stresses running along the axis of symmetry of the model.

Once the ball is unloaded, residual stresses will remain in the material of the cylindrical specimen. A map of the reduced residual stresses that remain in the specimen is given in Figure 9.

Figure 10 presents a diagram of reduced residual stresses along the axis of the cylindrical specimen. Maximum reduced stresses are 800 MPa, and occur at a depth of about 1 mm from the specimen surface.

The computations of Nastran FX also result in maps of plastic deformations that remain after the ball is unloaded. Figure 11 shows plastic deformation in a longitudinal section of the cylindrical specimen.

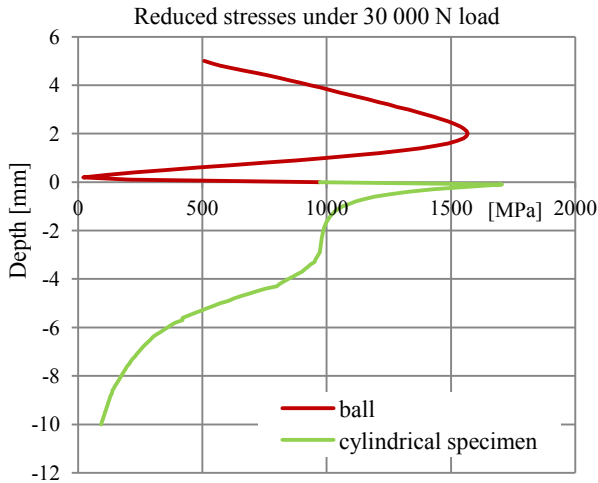


Figure 8. Reduced stresses in the ball and cylindrical specimen along the axis of symmetry under a 30,000 N load

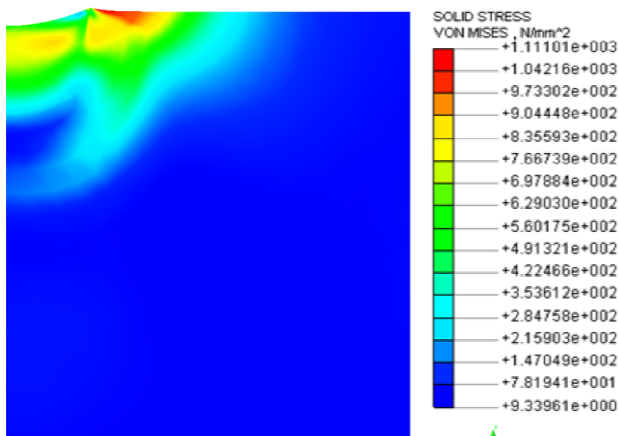


Figure 9. A map of reduced residual stresses that remain in the cylindrical specimen after the ball is unloaded

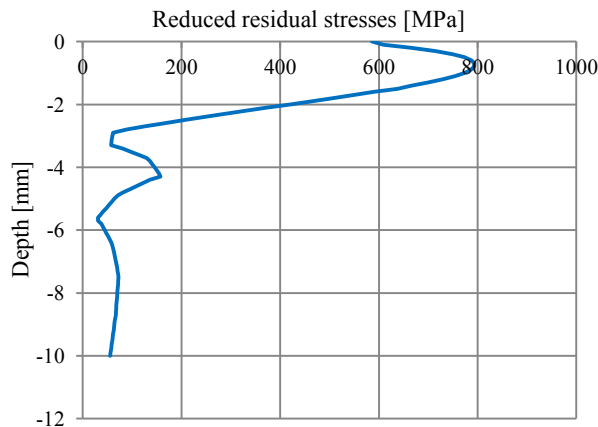


Figure 10. A diagram of reduced residual stresses along the specimen axis remaining in the material after ball unloading

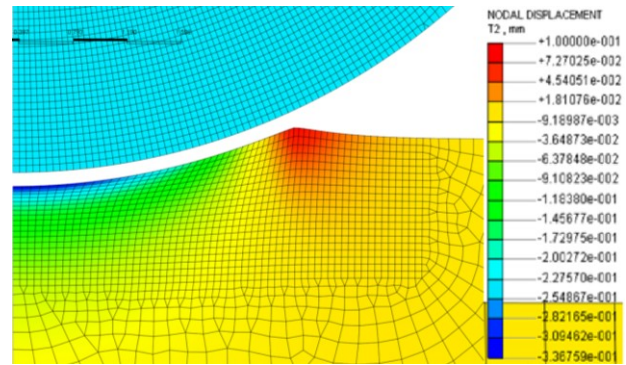


Figure 11. Deformations of the cylindrical specimen after ball unloading

The experiments

Indentations (Figure 12) made on the surface of steel specimens in hardness tests by the Brinell method (ceramic ball with a diameter of 10 mm, pressure force 30,000 N) were measured in a multi-sensor machine for surface topography measurements AltiSurf A520 (Sn/No:0513-A520-05/144), which has a confocal sensor CL2, measuring range of 400 μm and resolution of 22 nm. The cloud of points obtained was processed using AltiMap Premium software (version: 6.2.7200). The results of diameter and indentation depth h are compared in Figure 13.

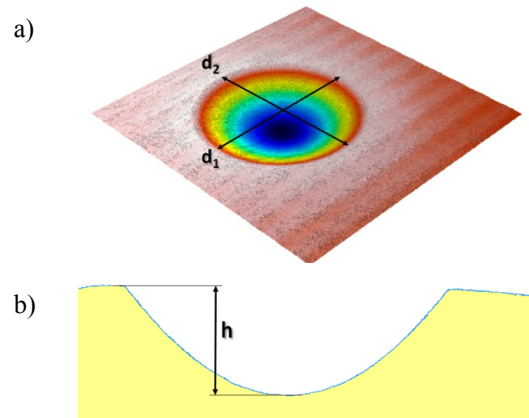


Figure 12. Deformations of the cylindrical specimen after ball unloading, a) view of the scanned surface and the method of indentation diameter measurement, b) indentation depth measurement (as per ISO 5436-1)

To verify the correctness of the results, only the plastic strains were checked. The indentation diameter and depth measurement results are plotted in Figure 13. The plots show a comparison of plastic deformations determined by Nastran FX (FEM), with a shape created after the pressing of an ideal 10 mm ball. The indentations from experiments and simulations display very good agreement. On this basis we can state that the distribution of residual stresses is also correct.

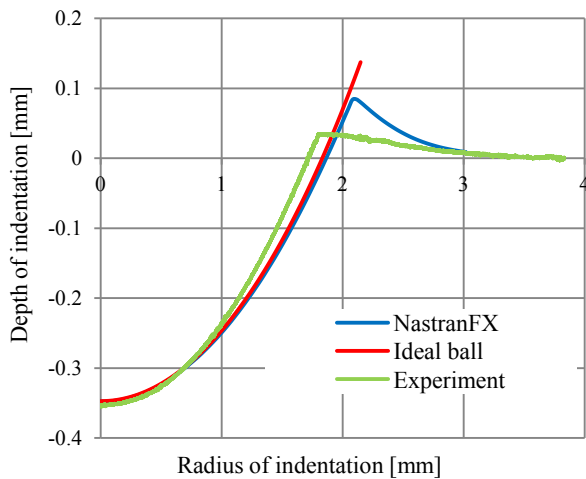


Figure 13. Comparison of the test results, shape of the radius and depth of the indentation

Conclusions

Developed in the Nastran FX software, a model of pressing a ceramic ball into elastic-plastic material may be used in further research into the optimization of technological burnishing parameters, and for simulation of the values and distributions of surface stresses in objects subjected to burnishing.

A computer model of a ball-flat surface contact requires a densified division by finite elements in the area of the point of contact.

Maximum values of reduced stresses in the elastic and plastic ranges occur under the material surface.

Preliminary calculations in the elastic range can be performed by a user-friendly program HertzWin that produces the results instantly.

Modern programs based on the finite elements method very accurately calculate plastic deformations. Experimental verification of residual stresses, although possible by X-ray methods, is very inconvenient (Senczyk, 2005).

References

- BUDYNAS, R. & NISBETT, K. (2008) *Shigley's Mechanical Engineering Design*. 8th edition. McGraw-Hill.
- DEEG, E.W. (1992) New algorithms for calculating hertzian stresses, deformations, and contact zone parameters. *AMP Journal of Technology*. 2. November. pp. 14–24.
- GROCHAŁA, D. (2011) *Nagniatanie narzędziami hydrostatycznymi powierzchni przestrzennych złożonych na frezarkach CNC*. Dissertation, West Pomeranian University of Technology, Szczecin
- GROCHAŁA, D., BERCZYŃSKI, S. & GRZĄDZIEL Z. (2014) Stress in the surface layer of objects burnished after milling. *International Journal of Advanced Manufacturing Technology*. 72. pp. 1655–1663.
- LOPEZ de LACALLE, L.N., LAMIKIZ, A., MUNOJA, J. & SANCHEZ J.A. (2005) Quality improvement of ball-end milled sculptured surfaces by ball burnishing. *International Journal of Machine Tools and Manufacture*. 45. pp. 1659–1668.
- LOPEZ de LACALLE, L.N., LAMIKIZ, A., SANCHEZ, J.A. & ARANA J.L. (2007) The effect of ball burnishing on heat-treated steel and inconel 718 milled surfaces. *International Journal of Machine Tools and Manufacture*. 32. pp. 958–968.
- Nastran FX (2010) [Online] Available from: <http://midasfea.se/mechanical.php> [Accessed: 7 July 2015]
- SENCZYK, D. (2005) *Podstawy tensometrii rentgenowskiej*. Poznań: Wydawnictwo Politechniki Poznańskiej.
- Vink System Design & Analysis (2015) [Online] Available from: <http://en.vinksd.nl/toolkit-mechanical-calculations/hertz-contact-stress-calculations> [Accessed: 7 July 2015]